Continuous-wave optical parametric oscillator pumped by a fiber laser green source at 532 nm

G. K. Samanta,[1,*] S. Chaitanya Kumar,[1] Ritwick Das,[1] and M. Ebrahim-Zadeh[1,2]

[1]*ICFO–Institut de Ciencies Fotoniques, Mediterranean Technology Park, 08860 Castelldefels, Barcelona, Spain*
[2]*Institucio Catalana de Recerca i Estudis Avancats (ICREA), Passeig Lluis Companys 23, Barcelona 08010, Spain*
**Corresponding author: goutam.samanta@icfo.es*

Received April 3, 2009; revised June 6, 2009; accepted June 10, 2009;
posted June 30, 2009 (Doc. ID 109674); published July 17, 2009

We report a high-power, cw, singly resonant optical parametric oscillator (SRO) using a simple, compact fiber pump laser architecture in the green. The SRO, based on MgO:sPPLT, is pumped by 9.6 W of single-frequency cw radiation at 532 nm obtained by single-pass second-harmonic generation (SHG) of a 30 W Yb fiber laser, also in MgO:sPPLT. Using two identical crystals of 30 mm length for SHG and SRO, we generate cw idler powers of up to 2 W over 855–1408 nm, with a peak-to-peak power stability <11.7% over 40 min, in a TEM_{00} spatial mode with $M^2<1.26$. Using finite output coupling of the resonant wave, we extract 800 mW of signal power with peak-to-peak power stability <10.7% over 40 min, and a frequency stability <75 MHz over 15 min. The signal and idler output have TEM_{00} beam profile with $M^2<1.52$ across the tuning range. © 2009 Optical Society of America

OCIS codes: 190.4970, 190.2620, 140.3510, 190.4360, 190.4400.

Continuous-wave, singly resonant optical parametric oscillators (SROs) are versatile sources of high-power, tunable, single-frequency radiation in spectral regions inaccessible to lasers. The advent of periodically poled $LiNbO_3$ (PPLN) with high optical nonlinearity ($d_{eff}\sim 17$ pm/V), interaction lengths up to 80 mm, and noncritical phase matching (NCPM) has had an unprecedented impact on cw SROs. Together with advances in solid-state pump lasers at 1064 nm, this has led to the realization of a new generation of cw SROs for the near IR and mid-IR [1], addressing various spectroscopic applications [2]. More recently, the introduction of alternative materials such as MgO-doped stoichiometric periodically poled $LiTaO_3$ (MgO:sPPLT), offering increased resistance to photorefractive damage, moderate nonlinearity ($d_{eff}\sim 10$ pm/V), and interaction lengths >20 mm under NCPM, has enabled the development of cw SROs below 1 μm [3–5], using high-power, frequency-doubled, cw solid-state lasers at 532 nm.

At the same time, for further progress in cw SROs, it is imperative to devise new architectures to reduce system complexity and cost while maintaining or enhancing device performance with regard to all important operating parameters. A major step in this direction is the development of more simplified pump sources based on the rapidly advancing fiber laser technology to replace the relatively complex and expensive cw solid-state lasers. This approach has already been successfully realized with cw fiber pump lasers at 1064 nm in combination with PPLN [6–8]. However, to our knowledge, extension of cw fiber laser technology to the green to pump visible and near-IR cw SROs [3–5] has so far not been feasible because of the difficulty in achieving sufficient green power with the required characteristics and in a simplified design. Here, we demonstrate what we believe to be the first cw SRO using a fiber laser green pump, realized by efficient single-pass second-harmonic generation (SHG) of a cw Yb fiber laser in MgO:sPPLT [9].

The schematic of the experimental setup is shown in Fig. 1. The primary pump source is a cw Yb fiber laser [9], delivering up to 30 W of single-mode output at 1064 nm with a nominal linewidth of 89 kHz, and a frequency stability <120 MHz over 1 h and <50 MHz over 30 min. Single-pass SHG in a 30 mm MgO:sPPLT crystal ($\Lambda=7.97$ μm) provides 9.64 W of cw, single-frequency output at 532 nm at 32.7% efficiency, in a TEM_{00} spatial mode, with a peak-to-peak power stability of 9% over 13 h, and frequency stability <32 MHz over 30 min [9].

The input pump power and polarization to the SRO are controlled using a polarizing beam splitter and two half-wave plates. The MgO:sPPLT crystal for the SRO is identical to the SHG sample [9]. The crystal temperature is controlled using an oven with a stability of ±0.1°C. The crystal coatings, SRO ring cavity, and mirror coatings are identical to our earlier

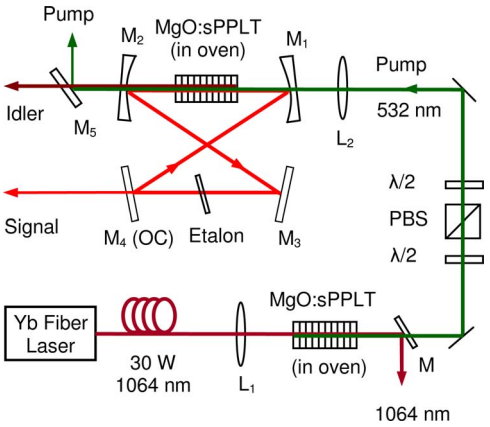

Fig. 1. (Color online) Schematic of experimental design for the fiber-laser-pumped MgO:sPPLT cw SRO. HWP, half-wave plate; PBS, polarizing beam splitter; M, mirror; L, lens.

work [3,5]. However, to maximize total power extraction and useful tuning range, we operate the device as an output-coupled (OC-) SRO [10], with mirror M_4 providing varying transmission ($T=0.71\%-1.1\%$) across the signal wavelength range. The pump waist at the center of the crystal is ~30 μm, with a corresponding signal waist of ~40 μm at 900 nm, resulting in optimum spatial overlap in the crystal ($b_s \sim b_p$). For frequency selection, a 500 μm uncoated fused silica etalon [FSR (free spectral range) =206 GHz, finesse ~0.6] is used at the second cavity waist. The total optical length of the cavity is 711 mm (FSR ~422 MHz).

The extracted signal and idler output power across the OC-SRO tuning range, obtained by varying the crystal temperature from 59°C to 236°C, is shown in Fig. 2. The device can simultaneously provide useful signal and idler power over a total tuning range of ~550 nm. Although we generate a green power of up to 9.64 W, the pump power available at the input to the OC-SRO crystal is 7.3 W, owing to unoptimized coatings of transmission optics. The outcoupled signal power, Fig. 2(a), varies from 725 mW at 1000 nm to 277 mW at 855 nm, with a maximum of 800 mW at 927 nm at the highest output coupling of 1.04% [10]. The corresponding idler power, Fig. 2(b), varies from 1.9 W at 1136 nm to 745 mW at 1408 nm, with a maximum power of 2.1 W at 1168 nm. As evident in Fig. 2(b), the idler power is nearly constant at ~1.8 W in the range of 1136–1252 nm, which is 42% of the total idler tuning range, and monotonically decreases toward the extreme of the tuning range owing to different factors, including thermal lensing at higher crystal temperatures and higher pump powers, as described previously [3,10]. However, unlike our earlier report on OC-SRO [10], here we generate more than 745 mW of idler power across the full tuning range, which is 1.5 times more than our previous results, and simultaneously extract over 300 mW of signal power. We attribute the increase in idler power to the lower pump and intracavity signal power density owing to looser focusing, resulting in reduced thermal effects. The pump depletion in the OC-SRO remains close to ~55% over most of the tuning range, before declining to ~34% at the extreme of the tuning range.

We recorded the power stability of the outcoupled signal at 971 nm and the corresponding idler at 1176 nm for a crystal temperature of 80°C, with the results shown in Figs. 3(a) and 3(b), respectively. The signal exhibits slightly higher peak-to-peak power stability (10.7%) than the idler (11.7%) over 40 min. The power instability of the signal and idler can be attributed to the green pump power fluctuation, measured to be ~8% peak to peak [9], and also owing to the residual thermal effects in the cw OC-SRO crystal.

We verified single-frequency nature of the generated signal and idler using a confocal interferometer (FSR=1 GHz, finesse ~400). The frequency stability of the outcoupled signal at 971 nm, measured at 600 mW using a wavemeter (High Finesse, WS/U-30), is shown in Fig. 4. The signal frequency exhibits a passive peak-to-peak stability <75 MHz over 15 minutes, with a nearly periodic variation in frequency deviation also evident with time. The inset of Fig. 4 shows the short-term frequency stability, where we can observe stable signal frequency to <10 MHz (limited by the relative accuracy of the wavemeter) over 10 s, before shifting to another frequency. We record similar behavior across the signal tuning range. The observed frequency instabilities are attributed to pump frequency jitter, pump and intracavity-signal-induced thermal noise, mechanical vibration of the experimental setup, and jitter of the measurement instrument (wavemeter). We expect the frequency stability of the system can be further enhanced with active stabilization and improved temperature stability of both crystals below ±0.1°C. This should also minimize the long-term drift in signal frequency also evident in Fig. 4. Owing to the limited spectral response of our wavemeter, we could not record the frequency stability of the nonresonant idler. However, we believe that the idler will not exhibit higher stability than the signal owing to the frequency fluctuations of the green pump [9].

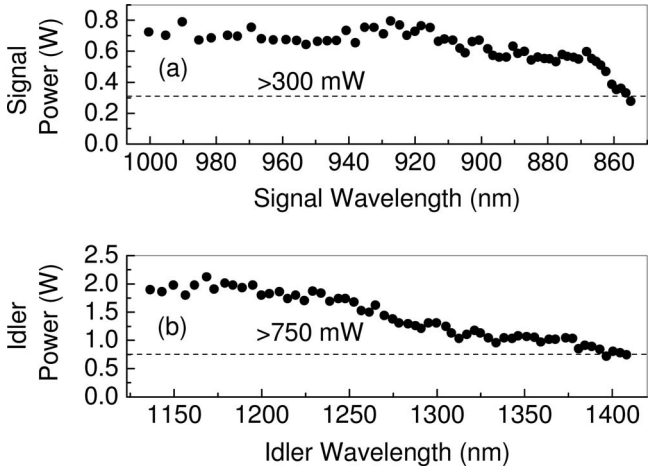

Fig. 2. Simultaneously extracted (a) signal power and (b) idler power, across the cw OC-SRO tuning range. Green pump power is 7.3 W.

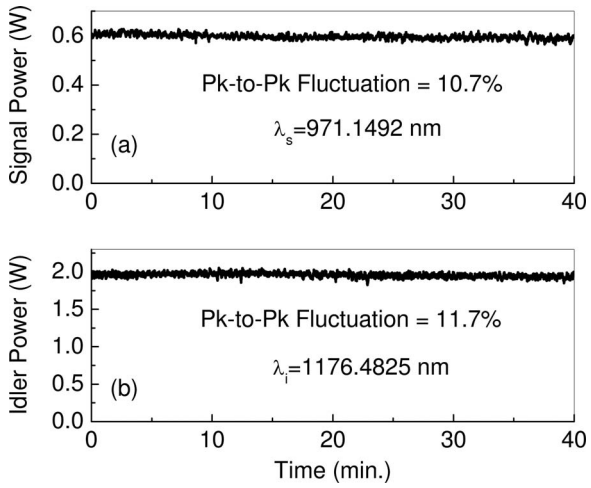

Fig. 3. Power stability of (a) outcoupled signal and (b) idler over 40 min. The crystal temperature is 80 °C.

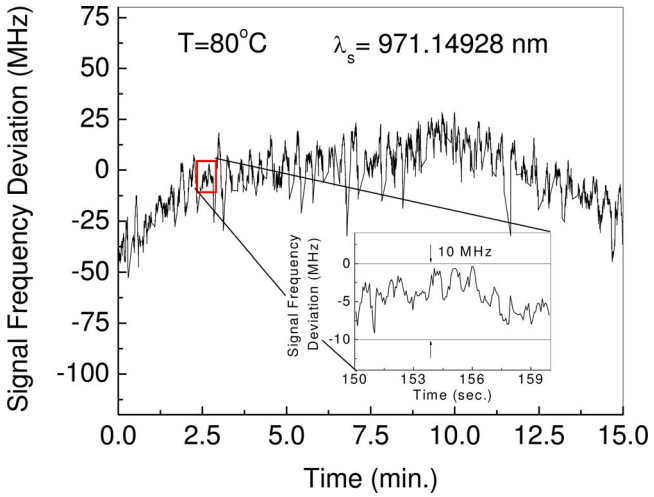

Fig. 4. (Color online) Long-term frequency stability of signal at wavelength 971.14928 nm for crystal temperature of 80°C over 15 min and (inset) short-term frequency stability over 10 sec.

The far-field energy distribution of the output signal beam at 971 nm, measured at a distance >2 m from the OC-SRO, together with the intensity profiles and the Gaussian fits, are shown Fig. 5. We measured M^2 factor of the signal and idler beams at the highest available pump power for five different crystal temperatures from 80°C to 200°C in 30°C intervals, using a $f=25$ cm focusing lens and scanning beam profiler. The results are shown in Fig. 6. The M^2 values for the signal were found to increase from $M_x^2 \sim 1.13$, $M_y^2 \sim 1.13$ at 80°C (971 nm) to $M_x^2 \sim 1.52$, $M_y^2 \sim 1.47$ at 200°C (874 nm). For the corresponding idler, the M^2 values were comparable with the pump ($M_x^2 \sim 1.28$, $M_y^2 \sim 1.24$), with a small variation in M_x^2 from 1.26 to 1.18 and M_y^2 from 1.26 to 1.12 across the tuning range. The increase in M^2 value of the signal beam with crystal temperature signifies thermal lensing effects in the OC-SRO at higher crystal temperatures [3].

In conclusion, we have demonstrated a cw SRO using a fiber laser pump source in the green and continuously tunable across 855–1408 nm. For 7.3 W of green pump power, the OC-SRO provides up to 2 W

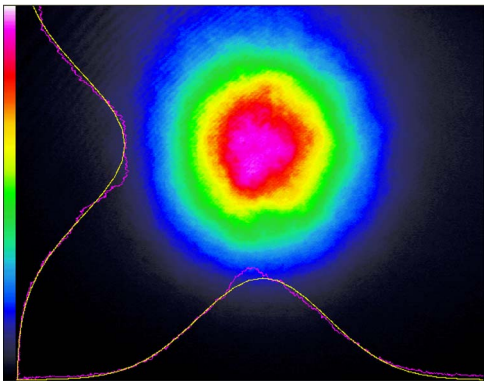

Fig. 5. (Color online) Far-field TEM_{00} energy distribution and intensity profiles of the generated signal beam at crystal temperature 80°C (971 nm) recorded at a distance >2 m away from OC-SRO.

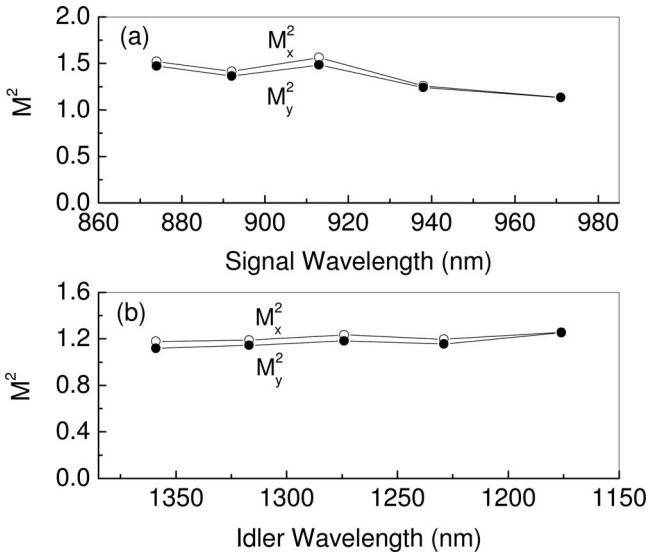

Fig. 6. Variation of M^2 for (a) signal and (b) idler across the tuning range of OC-SRO.

of idler in TEM_{00} spatial mode ($M^2<1.26$) with a peak-to-peak stability <11.7% over 40 min. With nonoptimum output coupling ($T=1.04\%$), up to 800 mW of signal power has been extracted in a TEM_{00} profile ($M^2<1.52$) with a peak-to-peak stability <10.7% over 40 min. The resonant signal exhibits a passive frequency stability of <75 MHz over 15 min and <10 MHz over 10 s. Using higher cw fiber power, improved transmission optics, optimized output coupling, and reduced thermal lensing with loose pump focusing, further improvements in output power and stability across the tuning range should be feasible.

This work was supported by the Ministry of Education and Science of Spain through grant TEC2006-12360 and the Consolider Project, SAUUL (CSD2007-00013). We also acknowledge partial support by the European Union 7th Framework Program, MIRSURG (224042).

References

1. W. R. Bosenberg, A. Drobshoff, J. I. Alexander, L. E. Myers, and R. L. Byer, Opt. Lett. **21**, 1336 (1996).
2. S. M. Cristescu, S. T. Persijn, S. Te Lintel Hekker, F. J. M. Harren, Appl. Phys. B **92**, 343 (2008).
3. G. K. Samanta, G. R. Fayaz, and M. Ebrahim-Zadeh, Opt. Lett. **32**, 2623 (2007).
4. J.-M. Melkonian, T.-H. My, F. Bretenaker, and C. Drag, Opt. Lett. **32**, 518 (2007).
5. G. K. Samanta and M. Ebrahim-Zadeh, Opt. Lett. **33**, 1228 (2008).
6. P. Gross, M. E. Klein, T. Walde, K.-J. Boller, M. Auerbach, P. Wessels, and C. Fallnich, Opt. Lett. **27**, 418 (2002).
7. I. Lindsay, B. Adhimoolam, P. Gross, M. Klein, and K. Boller, Opt. Express **13**, 1234 (2005).
8. A. Henderson and R. Stafford, Opt. Express **14**, 767 (2006).
9. G. K. Samanta, S. C. Kumar, and M. Ebrahim-Zadeh, Opt. Lett. **34**, 1561 (2009).
10. G. K. Samanta and M. Ebrahim-Zadeh, Opt. Express **16**, 6883 (2008).